Sakurai. *Chem Synth* 2024;4:42
DOI: 10.20517/cs.2023.76

Chemical Synthesis

Research Article

Open Access

Check for updates

On-surface synthesized magnetic nanoclusters of ferrocene derivatives

Makoto Sakurai*

International Center of Materials Nanoarchitectonics (WPI-MANA), National Institute for Materials Science (NIMS), Tsukuba 305-0044, Japan.

***Correspondence to:** Dr. Makoto Sakurai, International Center of Materials Nanoarchitectonics (MANA), National Institute for Materials Science (NIMS), 1-1 Namiki, Tsukuba 305-0044, Japan. E-mail: sakurai.makoto@nims.go.jp

How to cite this article: Sakurai M. On-surface synthesized magnetic nanoclusters of ferrocene derivatives. *Chem Synth* 2024;4:42. https://dx.doi.org/10.20517/cs.2023.76

Received: 29 Dec 2023 **First Decision:** 4 Jun 2024 **Revised:** 17 Jun 2024 **Accepted:** 2 Jul 2024 **Published:** 1 Aug 2024

Academic Editor: Yann Garcia **Copy Editor:** Pei-Yun Wang **Production Editor:** Pei-Yun Wang

Abstract

On-surface molecular self-assembly in solution can produce two-dimensional (2D) materials with unique surface nanostructures that have the potential to create new functionalities. The surface completely differs from the uniform flat surface of conventional 2D materials such as graphene, MoS_2, and 2D van der Waals nanosheets. The recently developed on-surface chemical synthesis of amino-ferrocene (AFc) nanoclusters on a graphene oxide (GO) nanosheet is a technique based on molecular self-assembly. Here, this method is applied to other ferrocene derivatives whose ferrocene units are covalently bonded to an amino group and several other molecules. The structure of the on-surface synthesized nanoclusters is analyzed by high-resolution transmission electron microscopy and atomic force microscopy. The molecules in the nanoclusters are densely and regularly arranged, and the distance between the Fe ions of the constituent molecules is longer than that in the AFc nanoclusters. Band-through electron transfer occurs between the Fe ions and the GO nanosheet, generating unpaired 3d electrons whose magnetic state is in the high spin state (S = 5/2). The present study demonstrates the feasibility of the design and synthesis of functional molecular nanostructures with molecular precision by on-surface chemistry, leading to the fabrication of nanoscale building blocks with molecular precision and 2D platforms for next-generation molecular spintronic and neuromorphic devices.

Keywords: On-surface chemistry, ferrocene derivative, nanocluster, high spin state, charge transfer, 2D materials

INTRODUCTION

Low-dimensional magnetism involves fundamental issues related to the formation of magnetic order and new phases due to the reduction of its dimensionality[1,2] and has been studied both experimentally and theoretically for many years[3-6]. Recently, two-dimensional (2D) materials, such as 2D van der Waals magnets[6-8], have been associated with the elucidation of order formation in the 2D limit[9] and have been applied to topological quantum computation[10]; they have revealed new physical phenomena such as the quantum Hall effect[11] and the quantum spin liquid[12]. These 2D materials are typically prepared by mechanical exfoliation of bulk layered materials[13]. On the other hand, the use of on-surface chemistry such as charge transfer, surface diffusion, and on-surface synthesis to fabricate functional nanosheets in solution is a bottom-up approach and is based on molecules diffusing on the surface in a self-assembled manner[14]. This method can arrange molecules with molecular-scale precision and form nanoscale molecular architectures whose precision and arrangement are difficult to fabricate using the top-down approach. The recently developed method of creating 2D materials using graphene oxide (GO) on-surface chemistry[15] is an example of this technique. Using coupling agents, an amino group attached to a ferrocene molecule and a carboxyl group on a GO nanosheet form covalent bonds, and the molecule bonded to the nanosheet acts as a nucleus for crystal growth of diffusing molecules on the nanosheets, leading to the formation of 2D materials with nanoscale molecular aggregates[15,16].

A ferrocene molecule is known to be a structurally and chemically stable unit whose Fe ion is located between two cyclopentadienyl rings and is in the zero magnetic state (S = 0) due to the paired 3d electrons[17]. An amino-ferrocene (AFc) molecule is formed by adding an amino group to the unit and has the same magnetic state (S = 0) as the ferrocene molecule[16]. After the on-surface chemical reaction, the Fe ions in the AFc molecules in the nanoclusters have unpaired electrons by charge transfer between the molecules and GO[15], and the 3d electrons of the Fe ions are in a high spin state (S = 5/2)[16]. The magnetic dipole interaction between the Fe ions in the nanoclusters affects their magnetic properties due to the short intermolecular distance and large magnetic moment[16]. In the present study, we applied this on-surface synthesis method to molecules whose ferrocene units are attached to amino groups and other additional molecules to investigate the growth, structure, and magnetic state of molecular assemblies on GO nanosheets, and to see how changing the Fe-Fe distance and nanocluster size affects the band-through charge transfer and the formation of the magnetic state of the ferrocene derivatives.

EXPERIMENTAL

Synthesis of ferrocene derivative-based assemblies

The on-surface chemical reaction of AFc molecules with GO nanosheets has already been reported[15]. In this process, nanoclusters of AFc molecules are formed on a GO nanosheet, where the coupling agents [1-(3-dimethylaminopropyl)-3-ethylcarbodiimide hydrochloride (EDC-HCl), 1-hydroxy-1-H-benzotriazode (HOBt), and trimethylpyridine] at low doses (≤ 0.1 mol/L) activate the covalent immobilization of the carboxyl group of the GO sheet and the amino group attached to the ferrocene unit in the ferrocene derivatives. In this study, 1 mL of water-dispersed GO solution (4 mg/mL) was mixed with 50 mL of *N*,*N*-dimethylformamide (DMF) solution, and they were stirred in a round-bottomed flask at 0 °C. Then, solid $C_{24}H_{24}FeNP$ molecules (20 mg, Sigma-Ardrich) or AFc (20 mg, TCI) and the coupling agents were added to the solution, which was stirred at 0 °C for three hours to control any excessive reaction in the initial stage of the synthesis. After the temperature of the solution was changed to about 24 °C, the solution was stirred for a given reaction time. The separation and washing processes after the synthesis were used to separate and purify the synthesized nanosheets, because there are many unreacted chemicals in the solution and on the nanosheets. The nanosheets in the solution were separated from the solution with unreacted chemicals by centrifugation. The washing process was used to remove unreacted chemicals on the

nanosheets using ~20 mL of DMF solution and resolve them out into the solution. This process was repeated several times. The nanosheets in the solution were further separated by centrifugation and washed with pure water or ethanol solution to remove DMF and other chemicals adsorbed on the nanosheets. This process was repeated two times and dried.

Characterization of the assemblies

The structure of the molecular assemblies on a GO nanosheet was investigated using a transmission electron microscope (TEM) (V-7200, JEOL) equipped with energy dispersive X-ray spectroscopy (EDX) and an atomic force microscope (AFM) (Dimension Icon, Bruker). First, 1-2 μL of diluted pure water solution containing the chemically synthesized nanosheets was dropped onto the TEM grid. After drying, the grid was placed on the TEM stage of the ultra-high vacuum (UHV) chamber for TEM observation [Figure 1A]. Additionally, 1-2 μL of dilute ethanol solution containing the nanosheets was dropped onto the SiO (90 nm)/Si substrate, and the dried substrate was used for AFM observation. The electronic states of the atoms forming the nanoclusters on the GO nanosheets were characterized by X-ray photoelectron spectroscopy (XPS) (Thermo Fisher Scientific Thera Probe system). The molecular components of the sheets were characterized by time-of-flight (TOF)-secondary ion mass spectrometry (SIMS) (PHI TRIFT V nanoTOF, Ulvac-Phi). A dense water solution containing the nanosheets was poured into a small hole in a clean copper thin plate. After drying, the aggregation of the sheets at the hole was measured by XPS and SIMS. The static magnetization and magnetic susceptibility under the application of a magnetic field were measured for aggregated nanosheets with a weight of 5-30 mg by using a superconducting quantum interference device (SQUID) magnetometer (MPMS-7T, Quantum Design).

RESULTS AND DISCUSSION

The GO nanosheets chemically reacted with ferrocene derivatives on a supporting carbon network of a TEM grid was observed by a TEM [Figure 1A]. Each sheet in the image is 2-10 μm long, and many folded areas and wrinkles are created during the on-surface chemical reaction and the subsequent separation, washing, and drying processes. The progress of the chemical reaction with ferrocene derivatives was monitored by measuring the amount of Fe atoms in the solution. After removing the chemically synthesized nanosheets from the solution at each reaction time by centrifugation, the amount of Fe atoms in the residual solution was measured using inductively coupled plasma optical emission spectroscopy (ICP-OES)[15]. The amount of Fe atoms measured by this method corresponds to the amount of unreacted ferrocene derivatives in the solution. The difference of this amount of Fe atoms from that in the initial solution corresponds to rough estimation of the amount of Fe atoms adsorbed on the GO nanosheets and is plotted as a function of reaction time [Figure 1B]. There is a large difference in the change between the reactions of $C_{24}H_{24}$FeNP molecules (inset of Figure 1C), in which aminoethyl and diphenylphosphino groups are attached to the ferrocene unit, with and without coupling agents. The increase in the amount of Fe atoms in the reaction of $C_{24}H_{24}$FeNP molecules with coupling agents (red open triangle) indicates that the reaction progresses and forms molecular assemblies on the GO nanosheets, similar to the reaction with AFc molecules (inset of Figure 1D) using the agents (blue open circle)[15]. The negligible change in the reaction without the agents (red open circle) indicates negligible adsorption of the molecules on the GO nanosheets. Hereinafter, the GO nanosheets reacted with $C_{24}H_{24}$FeNP molecules and coupling agents will be abbreviated as $C_{24}H_{24}$FeNP-GO sheets, and the nanosheets reacted with AFc molecules (inset of Figure 1D) and coupling agents for 24 h will be abbreviated as AFc-GO sheets.

The structure of a $C_{24}H_{24}$FeNP-GO sheet (reaction time: 96 h) and an AFc-GO sheet (reaction time: 24 h) was investigated by a TEM [Figure 1C and D]. In their TEM images, there were several dark regions on the GO nanosheet. A TEM-EDX analysis of the $C_{24}H_{24}$FeNP-GO sheet showed that the Fe signal originated only

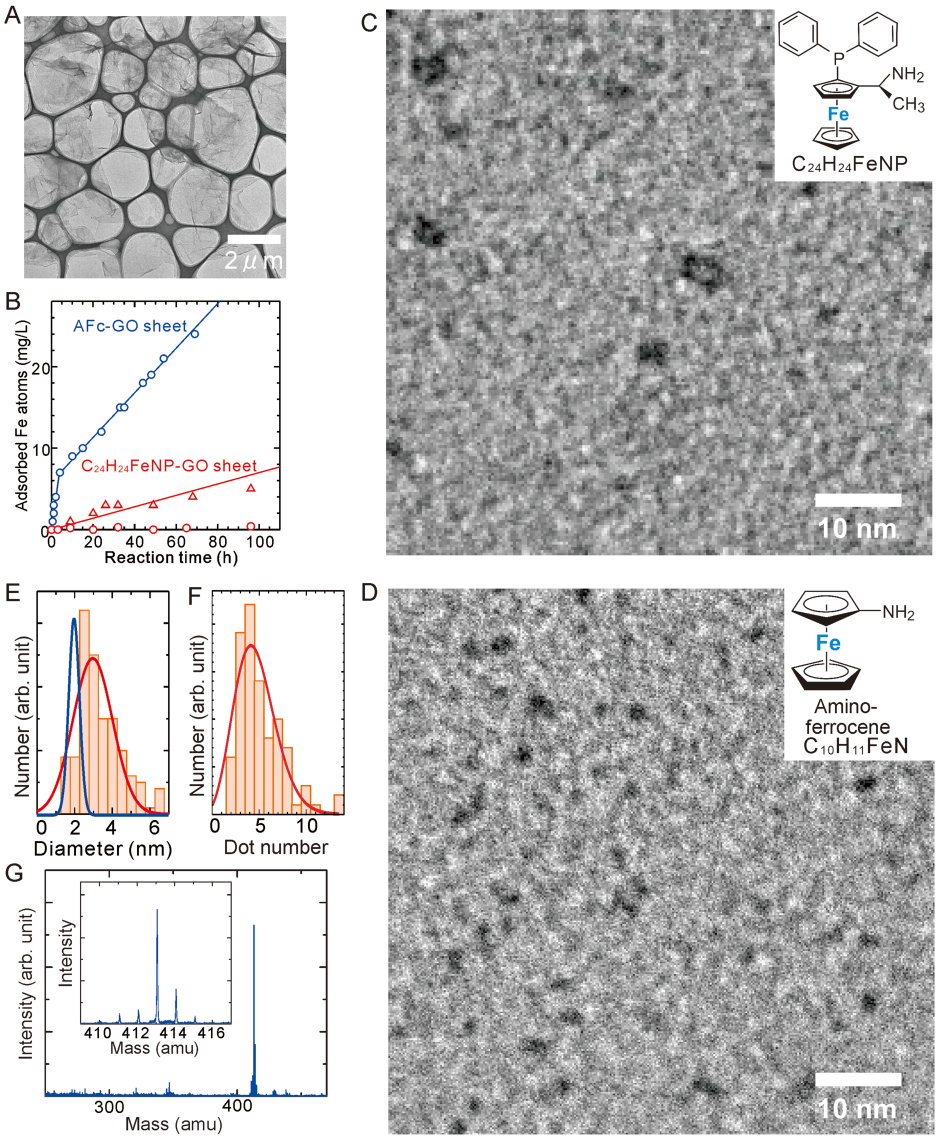

Figure 1. (A) A TEM image of several $C_{24}H_{24}$FeNP-GO sheets (reaction time: 96 h) on a supporting carbon network of the TEM grid; (B) The amount of Fe atoms adsorbed on the GO nanosheets as a function of reaction time for chemical reaction of $C_{24}H_{24}$FeNP-GO sheets with (red open triangle) and without coupling agents (red open triangle) and AFc-GO sheets with coupling agents (blue open circle); (C) Inset: Molecular structures of the $C_{24}H_{24}$FeNP molecule. A TEM image of a GO nanosheet after chemical reaction of $C_{24}H_{24}$FeNP with coupling agents for 96 h; (D) Inset: Molecular structures of AFc molecule. A TEM image of a GO nanosheet after chemical reaction of AFc molecules with coupling agents for 24 h. Dark regions in (C and D) correspond to the nanoclusters of ferrocene derivatives; (E) Histogram of the diameter of $C_{24}H_{24}$FeNP-GO sheets (reaction time: 96 h). Red and blue solid lines show the Gaussian fit to the data for $C_{24}H_{24}$FeNP-GO and AFc-GO sheets; (F) Histogram of the number of nanoclusters in small areas of the $C_{24}H_{24}$FeNP-GO sheets using the quadra-count method; (G) TOF mass spectrum of $C_{24}H_{24}$FeNP-GO sheets. Inset: magnified spectrum at about 413 amu. TEM: Transmission electron microscope; GO: graphene oxide; AFc: amino-ferrocene; TOF: time-of-flight.

from the dark regions [Supplementary Figure 1]. In the histogram of the lateral size of the regions measured from several TEM images of $C_{24}H_{24}$FeNP-GO sheets (reaction time: 96 h) [Figure 1E], the data are fitted by a Gaussian curve. The distribution in the $C_{24}H_{24}$FeNP-GO sheets (red curve) is broader than that in the AFc-GO sheets (blue curve). The distribution in the $C_{24}H_{24}$FeNP-GO sheets is further analyzed using the quadra-count method[18], where a large area TEM image of the $C_{24}H_{24}$FeNP-GO sheet is divided into small equal areas and a histogram is constructed by counting the number of the dark regions in each small area. The

distribution is well fitted by a Poisson distribution (red solid line in Figure 1F), indicating that the regions are uniformly distributed on the nanosheet[19]. This is similar to that of the AFc assemblies on the GO nanosheets[15]. The TOF mass spectrum of the $C_{24}H_{24}$FeNP-GO sheets (reaction time: 96 h) had a peak at 413 amu [Figure 1G], which corresponds to the atomic weight (413.28 amu) of the $C_{24}H_{24}$FeNP molecule. This suggests that the $C_{24}H_{24}$FeNP molecules are assembled on the GO nanosheet without decomposition or oxidation, which would be due to the electronic stability of the ferrocene unit[19]. The satellite peaks around the main peaks in the spectrum (inset of Figure 1G) originate from the isotopic patterns[20]. Thus, it is concluded that the dark regions in the TEM image [Figure 1C] are assemblies of $C_{24}H_{24}$FeNP molecules. This is consistent with the finding that the dark regions in the AFc-GO sheets [Figure 1D] are formed by AFc molecules[15].

To confirm the shape of the molecular assemblies, the height of the $C_{24}H_{24}$FeNP molecular assemblies on the GO nanosheets (reaction time: 96 h) was measured using an AFM. The white dots in the topological AFM image correspond to the assemblies [Figure 2A]. The cross-sectional line profile of the $C_{24}H_{24}$FeNP assembly marked with the yellow triangle in Figure 2A is shown in Figure 2B. The lateral width of the dots in the AFM image was much larger than that in the TEM images due to the tip effect[21], because the curvature of the AFM tip (100-500 nm) is much larger than that of the assemblies. The histogram of the diameter and height of $C_{24}H_{24}$FeNP assembly synthesized using the coupling agents for 46 h is shown in Supplementary Figure 2. The height of the $C_{24}H_{24}$FeNP assembly has a wider distribution than that of AFc assembly[15] [Figure 2C and Supplementary Figure 2B]. The growth of the $C_{24}H_{24}$FeNP molecular assemblies on the GO nanosheet is similar to Volmer-Weber (VW) growth[22] because the molecules adsorbed on the surface diffuse along the surface. Such aggregates are hereafter referred to as nanoclusters. The size of the $C_{24}H_{24}$FeNP nanoclusters gradually increased with reaction time [Supplementary Figure 2, Figure 1E and 2C]. The nanocluster growth on the GO nanosheet is schematically shown in Figure 2D, where the molecule covalently bonded to the GO nanosheet acts as a nucleus for diffusing molecules in the formation of a nanocluster.

The distance between the Fe ions of the ferrocene derivatives in the nanocluster on a GO nanosheet was investigated by taking high-resolution (HR)-TEM images [Figure 3A and B] and performing a fast Fourier transform (FFT) [Figure 3C and D]. The atom-resolved patterns in the TEM images show a regular arrangement of molecules in the nanocluster. The arrangement is completely different from that of the bulk AFc crystal[23], because the surface of the GO nanosheet plays an important role in the formation of a nanocluster. The Fe atoms in the ferrocene derivatives have larger structure factors with respect to the incident electron beams of the TEM than those of the C, O, H, N, and P atoms in the ferrocene derivatives, the GO nanosheet, and the thin carbon support layers of the TEM grid. Thus, the atom-resolved patterns in the HR-TEM images [Figure 3A and B] reflect the regular arrangement of Fe ions in the ferrocene derivatives forming a nanocluster. From the spacing of the main spots in the FFT patterns [Figure 3C and D], the lateral lattice constants and the corresponding angles between them in each oblique system are 0.22 nm, 0.22 nm, and 96.3°, respectively, for the $C_{24}H_{24}$FeNP nanoclusters, and 0.20 nm, 0.20 nm, and 86.3°, respectively, for the AFc nanoclusters [Figure 3E and F]. The three-dimensional relationship of the Fe sites colored in blue and orange is schematically shown in Figure 3G. The lateral Fe-Fe distance in the $C_{24}H_{24}$FeNP nanocluster is longer than that in the AFc nanocluster. Since the lateral lattice constants of both nanoclusters are shorter than the distance (0.34 nm) between the two cyclopentadienyl rings of the ferrocene unit[24], the derivatives in the nanocluster are considered to be stacked with the rings nearly parallel to the GO surface. This analysis leads to the interpretation that the vertical stacking period of the molecules for the $C_{24}H_{24}$FeNP nanoclusters must be longer than that of the AFc nanoclusters due to the structural difference in their respective molecules (insets of Figure 1C and D). This leads to the conclusion

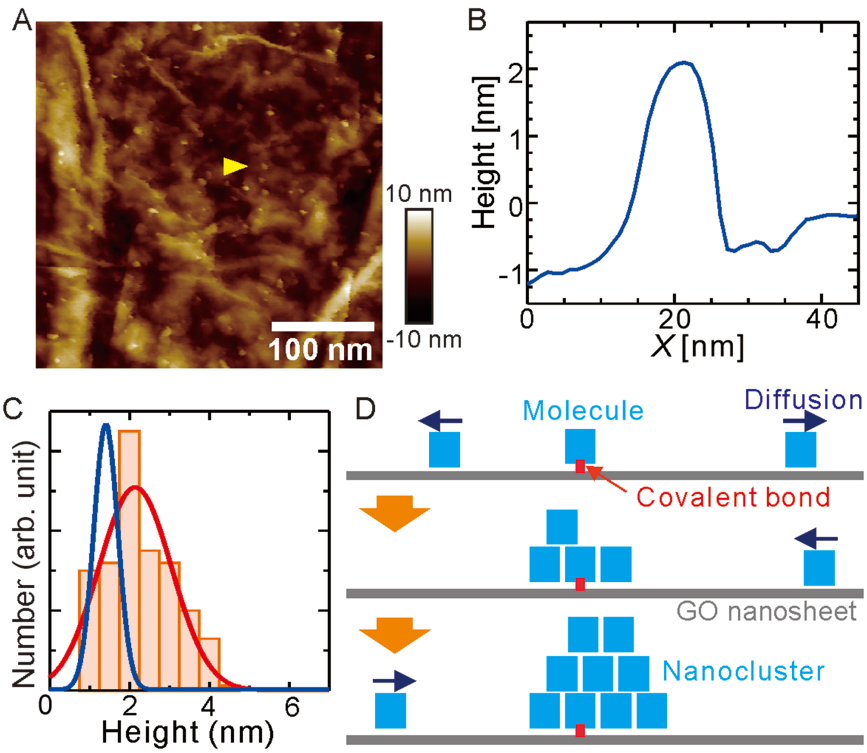

Figure 2. (A) A topological AFM image of $C_{24}H_{24}$FeNP nanoclusters on the GO nanosheet (reaction time: 96 h); (B) A cross-sectional line profile of the nanocluster marked with yellow triangle in (A); (C) Histogram of the heights of $C_{24}H_{24}$FeNP nanoclusters on the GO nanosheets (reaction time: 96 h). Red and blue solid lines show the Gaussian distribution fitted to the data for the $C_{24}H_{24}$FeNP-GO and AFc-GO sheets; (D) Schematic sequential illustration of the on-surface chemical reaction in which the molecule covalently bonded to the GO nanosheet acts as a nucleus for crystal growth. AFM: Atomic force microscope; GO: graphene oxide; AFc: amino-ferrocene.

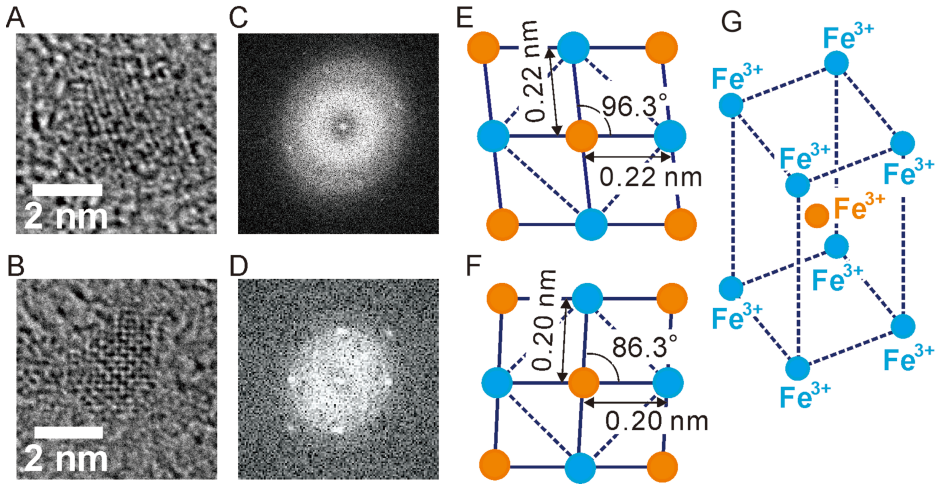

Figure 3. (A) High-resolution TEM images and (B) corresponding FFT patterns of a $C_{24}H_{24}$FeNP nanocluster on a GO nanosheet; (C) High-resolution TEM images and (D) corresponding FFT patterns of an AFc nanocluster on a GO nanosheet; The main spots of the FFT patterns correspond to the lateral molecular arrangement of Fe ions in the molecules shown schematically in (E) the $C_{24}H_{24}$FeNP and (F) the AFc nanocluster; (G) The fundamental unit of the lateral arrangement is formed three-dimensionally by the corresponding Fe ions (orange and blue dots). TEM: Transmission electron microscope; FFT: fast Fourier transform; GO: graphene oxide; AFc: amino-ferrocene.

that the distance between neighboring Fe ions in the nanoclusters can be tuned using ferrocene derivatives with additional molecular groups attached to the ferrocene units, while maintaining their crystallinity.

The investigation of the ionized state of Fe ions in the on-surface synthesized nanoclusters is instructive to study how the change in the Fe-Fe distance affects the band-through change transfer and the formation of the magnetic state. The electronic states of C and Fe atoms in the $C_{24}H_{24}$FeNP-GO sheets (reaction time: 96 h) were characterized by XPS [Figure 4A and B]. As the reaction progressed, the main peak of the C1s core level in the XPS spectra of the $C_{24}H_{24}$FeNP-GO sheets [Figure 4A] gradually shifted from the peak position of pristine GO nanosheets (~286.5 eV) to that of the $C_{24}H_{24}$FeNP molecules (~284.5 eV), where the peaks at 286.5 and 284.5 eV correspond to C–O–C and C–C bonds, respectively[25,26]. Since XPS signals are generated from the light emitted by the atoms forming the top surface[27], the gradual peak shift in the spectra is due to an increase in the ratio of $C_{24}H_{24}$FeNP molecules on the surface, supporting the growth of the nanoclusters composed of $C_{24}H_{24}$FeNP molecules. The peak positions of the Fe 2p core level in the spectra [Figure 4B] shifted after the reaction of $C_{24}H_{24}$FeNP molecules with the GO nanosheets, indicating that the ionized state of the Fe atoms in the $C_{24}H_{24}$FeNP molecules changed from Fe^{2+} to Fe^{3+}[28], which is due to band-through electron transfer from the molecule to the GO nanosheet, similar to the peak shift in the AFc-GO sheets caused by the charge transfer[15], where the GO nanosheet acts as electron acceptors. The change in the Fe/C ratio obtained from the spectra corresponds to an increase in the number of ferrocene derivatives with increasing reaction time [Figure 4C]. Note that the electron in the Fe ion of the ferrocene derivatives travels to the GO nanosheet along a longer path through several molecules in the $C_{24}H_{24}$FeNP nanocluster than in the AFc nanocluster, because the Fe-Fe distance in the $C_{24}H_{24}$FeNP nanoclusters is longer than that in the AFc nanoclusters and the $C_{24}H_{24}$FeNP nanoclusters are larger than the AFc nanoclusters. The transfer caused the Fe ions on the $C_{24}H_{24}$FeNP-GO sheets to have unpaired electrons, which is confirmed by the appearance of a large magnetization in the magnetization curve of the $C_{24}H_{24}$FeNP-GO sheets (reaction time: 96 h) at 2 K [Figure 4D]. This is completely different from that of the solid $C_{24}H_{24}$FeNP molecular powder (blue line in Figure 4D) in which the Fe ions are in the zero spin state ($S = 0$)[17].

The magnetic state of the Fe ions in the $C_{24}H_{24}$FeNP nanoclusters on a GO nanosheet was studied using the magnetic susceptibility $\chi_{M,FD}$ of the ferrocene derivative, which is simply expressed as M_{FD}/H where magnetization M_{FD} of the molecule is estimated using Equation (1) in Supplementary Materials. The $\chi^{-1}_{M,FD}$ of the molecule for both nanoclusters according to the Curie-Weiss law[29-31]: $\chi_{M,FD}(T) = C/(T - \Theta_{CW})$ are plotted as a function of T [Figure 4E]. The negative Θ_{CW} implies negative interactions between the molecular spins from the mean-field theory[32]. The linear relationship of the data at $T \geq 20$ K suggests that the molecular spins exhibit paramagnetic behavior at the temperature. The magnetic moment of the Fe ions in the nanoclusters was estimated from the linear slope by the Curie-Weiss law. The relationship between C and S is expressed as $C = g^2S(S + 1)\mu_B^2/3k_BW_{FD}$, where g is the g-factor and S is the spin quantum number[29,31]. The difference between the slopes in Figure 4E is mainly due to the different molecular weights W_{FD} ($C_{24}H_{24}$FeNP: 413.28, AFc: 201.05). Assuming g to be 2, the magnetic moments of the AFc and $C_{24}H_{24}$FeNP molecules on the nanosheets were calculated from each value of C [Figure 4E] to be 5.1 and 5.5 μ_B, respectively. These values are closer to the magnetic moment of the Fe^{3+} high spin state ($S = 5/2$), i.e., 5 μ_B, than to the magnetic moment of the Fe^{3+} low spin state ($S = 1/2$), i.e., 1 μ_B. This estimation of magnetic moment in AFc-GO sheets (reaction time: 24 h) is consistent with that in AFc-GO sheets (reaction time: 5 h)[16]. From these results, it is concluded that the 3d electrons of the Fe ions in both nanoclusters on the GO surface were in the high spin state ($S = 5/2$). Note that the low magnetic moment ($S = 1/2$) reported in ref.[15] resulted from an underestimation of the saturated magnetization by using the magnetization at $H = 70$ kOe in the unsaturated M-H loop of AFc-GO sheets at 2 K. It should be noticed that the high spin state ($S =$

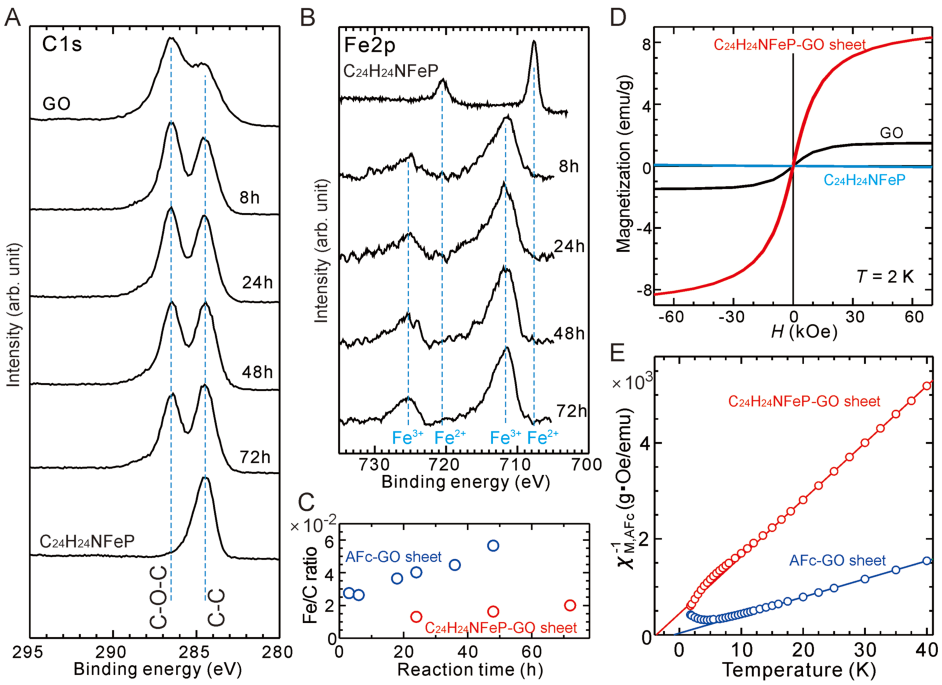

Figure 4. (A and B) A series of XPS spectra of C1s and Fe2p core levels of the $C_{24}H_{24}$FeNP-GO sheets as a function of reaction time; (C) The Fe/C ratios obtained from the XPS spectra of GO nanosheets reacted with $C_{24}H_{24}$FeNP (red open circle) and AFc molecules (blue open circle) as a function of reaction time; (D) Magnetization curves of $C_{24}H_{24}$FeNP-GO sheets (reaction time: 96 h), GO sheets, and solid $C_{24}H_{24}$FeNP molecular powder at 2 K; (E) $\chi_{FD}^{-1}(T)$ plotted against T for $C_{24}H_{24}$FeNP-GO (reaction time: 96 h) (red open circle) and AFc-GO (reaction time: 24 h) (blue open circle) sheets. The solid line showing linear fitting to the data according to the Currie-Weiss law. XPS: X-ray photoelectron spectroscopy; GO: graphene oxide; AFc: amino-ferrocene.

5/2) of the Fe ions in the $C_{24}H_{24}$FeNP nanocluster is formed by the band-through charge transfer, although the Fe-Fe distance in the nanocluster is enlarged by adding additional molecules in the ferrocene unit.

CONCLUSIONS

This study demonstrates the feasibility of self-assembled fabrication of functional nanoclusters using ferrocene derivatives in which an amino group and several other molecules are covalently bonded to the ferrocene unit. The present study shows that the molecule bonded by the covalent immobilization between the amino group of the $C_{24}H_{24}$FeNP molecule and the carboxyl group of the GO nanosheet under the coupling agents acts as a nucleus in the formation of on-surface synthesized nanoclusters with the regular molecular arrangement. A HR-TEM analysis shows that the Fe-Fe distance in the molecular nanoclusters can be tuned by using the ferrocene derivatives while maintaining their crystallinity. The present approach shows that band-through charge transfer occurs across several ferrocene derivatives to the GO nanosheet and that the 3d electrons of the Fe ions in the derivatives are in the high spin state (S = 5/2) for the nanoclusters whose size and Fe-Fe distance are increased by the on-surface chemical reaction of the ferrocene derivatives. The present results could provide guidance for the design and synthesis of attractive 2D materials using GO on-surface chemistry.

DECLARATIONS

Authors' contributions

The author contributed solely to the article.

Availability of data and materials
Not applicable.

Financial support and sponsorship
This work was supported by JSPS KAKENHI Grant name JP21K04821 and in part by the International Center of Materials Nanoarchitectonics (WPI-MANA), MEXT, Japan.

Conflicts of interest
The author declared that there are no conflicts of interest.

Ethical approval and consent to participate
Not applicable.

Consent for publication
Not applicable.

REFERENCES
1. Mermin ND, Wagner H. Absence of ferromagnetism or antiferromagnetism in one- or two-dimensional isotropic Heisenberg models. *Phys Rev Lett* 1966:17;1133-6. DOI
2. Kodama RH. Magnetic nanoparticles. *J Magn Magn Mater* 1999:200;359-72. DOI
3. Bruno P. Magnetization and Curie temperature of ferromagnetic ultrathin films: the influence of magnetic anisotropy and dipolar interactions (invited). *Proc MRS* 1991:231;299-310. DOI
4. Siegmann HC. Surface and 2D magnetism. *J Phys Condens Matter* 1992:4;8395. DOI
5. Rong C, Li D, Nandwana V, et al. Size-dependent chemical and magnetic ordering in $L1_0$-FePt nanoparticles. *Adv Mater* 2006:18;2984-8. DOI
6. Lee JU, Lee S, Ryoo JH, et al. Ising-type magnetic ordering in atomically thin $FePS_3$. *Nano Lett* 2016:16;7433-8. DOI PubMed
7. Gong C, Li L, Li Z, et al. Discovery of intrinsic ferromagnetism in van ver Waals crystals. *Nature* 2017:546;265-9. DOI PubMed
8. Huang B, Clark G, Navarro-Moratalla E, et al. Layer-dependent ferromagnetism in a van der Waals crystal down to the monolayer limit. *Nature* 2017:546;270-3. DOI PubMed
9. Deng Y, Yu Y, Song Y, et al. Gate-tunable room-temperature ferromagnetism in two-dimensional Fe_3GeTe_2. *Nature* 2018:563;94-9. DOI PubMed
10. Li J, Li Y, Du S, et al. Intrinsic magnetic topological insulators in van der Waals layered $MnBi_2Te_4$-family materials. *Sci Adv* 2019:5;eaaw5685. DOI PubMed PMC
11. Xue F, Hou Y, Wang Z, et al. Tunable quantum anomalous Hall effects in ferromagnetic van der Waals heterostructures. *Natl Sci Rev* 2023:11;nwad151. DOI PubMed PMC
12. Law KT, Lee PA. 1T-TaS_2 as a quantum spin liquid. *Proc Natl Acad USA* 2017:114;6996-7000. DOI PubMed PMC
13. Liu F. Mechanical exfoliation of large area 2D materials from vdW crystals. *Prog Surf Sci* 2021:96;100626. DOI
14. Dreyer DR, Todd AD, Bielawski CW. Harnessing the chemistry of graphene oxide. *Chem Soc Rev* 2014;43;5288-301. DOI PubMed
15. Sakurai M, Koley P, Aono M. Morphological change of molecular assemblies through on-surface chemical reaction. *J Phys Chem C* 2019:123;29679-85. DOI
16. Sakurai M, Ueta T, Joachim C. Weekly interacting molecular spins in on-surface synthesized nanoclusters on a graphene oxide nanosheet. *Adv Electron Mater* 2023;9;2300347. DOI
17. Crabtree RH. Pi-complexes. In: The organometallic chemistry of the transition metals. Wiley; 2014. pp. 134-62. DOI
18. Ripley BD. 2 - Likelihood analysis for spatial Gaussian processes. In: Statistical inference for spatial process. Cambridge University Press; 1991. pp. 9-21. DOI
19. Pauson PL. Ferrocene and related compounds. *Q Rev Chem Soc* 1955:9;391-414. DOI
20. Cervetti C, Rettori A, Pini MG, et al. The classical and quantum dynamics of molecular spins on graphene. *Nat Mater* 2016;15;164-8. DOI PubMed PMC
21. Keller DJ, Franke FS. Envelope reconstruction of probe microscope images. *Sur Sci* 1993:294;409-19. DOI
22. Zangwill A. 15 - Surface reactions. In: Physics at surfaces. Cambridge univ. Press; 1988. pp. 400-20. DOI
23. Perrine CL, Zeller M, Woolcock J, Hunter AD. Crystal structure of ferrocenyl amine. *J Chem Crystal* 2005:35;717-21. DOI

24. Haaland A. Molecular structure and bonding in the 3d metallocenes. *Acc Chem Res* 1979:12;415-22. DOI
25. Ren PG, Yan DX, Ji X, Chen T, Li ZM. Temperature dependence of graphene oxide reduced by hydrazine hydrate. *Nanotechnology* 2011;22:055705. DOI PubMed
26. Perrozzi F, Prezioso S, Ottaviano L. Graphene oxide: from fundamentals to applications. *J Phys Cond Matter* 2015;27:013002. DOI PubMed
27. Lüth H. Electronic surface states. In: Surfaces and interfaces of solid materials. Berlin: Springer. 1995. pp. 254-315. DOI
28. Yamashita T, Hayes P. Analysis of XPS spectra of Fe^{2+} and Fe^{3+} ions in oxide materials. *Appl Surf Sci* 2008;254;2441-9. DOI
29. Kahn O. Chapter 2 - Molecules containing a unique magnetic center without first-order orbital momentum. In: Molecular magnetism. VCH; 1992. Available from: https://www.scribd.com/document/382790790/Kahn-Molecular-Magnetism. [Last accessed on 12 Jul 2024].
30. Morrish AH. Chapter 3 - Thermal, relaxation, and resonance phenomena in paramagnetic materials. In: The physical principles of magnetism. Wiley; 1965. pp. 78-148. DOI
31. Miller JS, Epstein AJ, Reiff WM. Ferromagnetic molecular charge-transfer complexes. *Chem Rev* 1988:88;201-20. DOI
32. Skomski R. Chapter 2 - Models of exchange. In: Simple models of magnetism. Oxford: Oxford University press; 2008. pp. 15-72. DOI